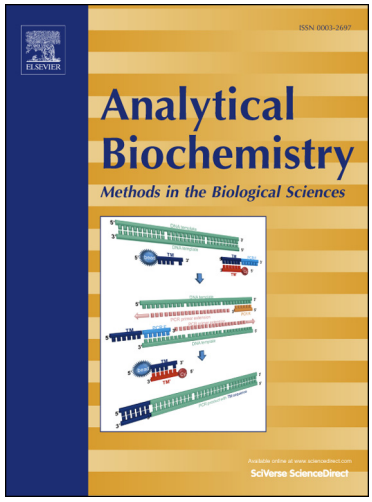

An electrochemical DNA biosensor based on gold nanorods decorated graphene oxide sheets for sensing platform

Xiaowei Han, Xian Fang, Anqi Shi, Jiao Wang, Yuzhong Zhang

PII: S0003-2697(13)00411-9
DOI: http://dx.doi.org/10.1016/j.ab.2013.08.027
Reference: YABIO 11478

To appear in: *Analytical Biochemistry*

Received Date: 21 May 2013
Revised Date: 12 August 2013
Accepted Date: 28 August 2013

Please cite this article as: X. Han, X. Fang, A. Shi, J. Wang, Y. Zhang, An electrochemical DNA biosensor based on gold nanorods decorated graphene oxide sheets for sensing platform, *Analytical Biochemistry* (2013), doi: http://dx.doi.org/10.1016/j.ab.2013.08.027

An electrochemical DNA biosensor based on gold nanorods decorated graphene oxide sheets for sensing platform

Xiaowei Han, Xian Fang, Anqi Shi, Jiao Wang, Yuzhong Zhang*

College of Chemistry and Materials Science, Anhui Normal University, Wuhu 241000, People's Republic of China

Subject category: Nucleic acids & Biosensor

Short title: Gold nanorods decorated graphene sheets for DNA detection

* Corresponding author. Tel.: +86 553 3869303; Fax: +86 553 3869303

E-mail address: zhyz65@mail.ahnu.edu.cn (Y. Zhang).

Abstract

A simple electrochemical sensor for sensitive and selective DNA detection was constructed based on gold nanorods (Au NRs) decorated graphene oxide sheets (GO). The high-quality Au NRs-GO nanocomposite was synthesized via the electrostatic self-assembly technique, which is considered as potential sensing platform. Differential pulse voltammetry was utilized to monitor the DNA hybridization event using methylene blue as an electrochemical indicator. Under optimum conditions, the peak currents of methylene blue were linear with the logarithm of the concentrations of complementary DNA from 1.0×10^{-9} to 1.0×10^{-14} M with a detection limit of 3.5×10^{-15} M (S/N=3). Moreover, the prepared electrochemical sensor can effectively distinguish complementary DNA sequences in the presence of a large amount of single-base mismatched DNA (1000:1), indicating that the biosensor has high selectivity.

Keywords: Gold nanorods, Graphene oxide, DNA biosensor, Differential pulse voltammetry

Rapid, simple, sensitive and selective DNA analysis has been attracted ever-increasing attentions in many fields, including molecular diagnostics, environmental monitoring, clinical diagnosis, and forensic analysis [1-4]. Therefore, many techniques have been developed for DNA detection such as surface-enhanced Raman scattering [5], surface plasmon resonance spectroscopy [6], electrochemical [7, 8] and fluorescence [9]. Among them, electrochemical method has been widely used due to its high sensitivity, simplicity, rapidness and low cost. Recently, various nanostructures have been employed as novel sensing platform due to their unique merits (e.g., large surface-to-volume ratio, excellent electronic/mechanical/catalytic properties, etc), which have been extensively applied in constructing DNA sensor. For example, Fan and co-workers [10] have reported a chronocoulometric DNA sensor via gold nanoparticles (Au NPs) amplification, which can detect as low as 10 fM DNA. Wang's group [11, 12] has fabricated several nanomaterials-based electrochemical sensors, which significantly enhanced the sensitivity and selectivity of DNA detection. Our group [13] has employed Au NPs /poly(L-lysine) complex film to fabricate a chronocoulometric sensor for the detection of DNA.

Over the past two decades, Au NPs have received widespread interest in the detection of DNA because of its unique optical, electronic properties and excellent biocompatibility. Following the pioneering work of Mirkin and co-workers [14, 15], more and more researchers focused on DNA detection using spherical Au NPs [16]. Gold nanorods (Au NRs) possess general properties similar to Au NPs and have several advantages over the spherical Au NPs such as faster electron-transfer ability, higher surface area and stronger light scattering properties [17, 18]. The application of Au NRs as sensing platform for DNA detection has been exploited [19, 20]. For example, Huang and co-workers [21] have reported an Au NRs-based optical biosensor for the detection of sequence-specific DNA, which related to the human immunodeficiency virus. Our group [22] has also reported a sensitive fluorimetric biosensor for detection of hepatitis B virus based on fluorescence resonance energy transfer between Au NRs and fluorescein, which could detect as low as 15 pM target DNA. As well known, graphene oxide (GO) has larger surface area, excellent biocompatibility, high water-soluble, and exceptional fluorescence-quenching ability, which has been used for DNA and biomolecules sensing [9, 23, 24]. For example, Chen and co-workers [25] have fabricated a colorimetric biosensor to detect heparin based on AuNRs -GO nanocomposite. Because the surface of GO contains abundant carbonyl and carboxy groups, so its surface has

large numbers of negative charges. Meanwhile, Au NRs were synthesized according to the seed-mediated and cetyltrimethy lammonium bromide (CTAB) surfactant-directed method, suggesting CTAB-stabilized Au NRs contain numerous positive charges. Therefore, Au NRs-GO nanocomposite can be easily prepared via the electrostatic self-assembly technique. Inspired from the application of Au NRs-GO nanocomposite, we select Au NRs-GO nanocomposite as sensing platform for the detection of specific sequences DNA in this study. Compared with bare electrode, the Au NRs-GO nanocomposite greatly improves the surface area of the electrode and loaded more probe DNA. The sensitivity of the DNA biosensor has obviously improved. Moreover, the biosensor shows high selectivity, stability and reproducibility for DNA detection. The fabrication procedure of DNA biosensor is shown in Scheme 1.

Scheme 1

Materials and methods

Reagents

Graphite oxide (GO) was obtained from Nanjing XFNano Materials Tech Co., Ltd., (Nanjing, China). Chloroauric acid ($HAuCl_4.4H_2O$) and methylene blue (MB) were obtained from Shanghai Chemical Reagent Co., Ltd. Cetyltrimethylammonium bromide (CTAB), silver nitrate ($AgNO_3$), sodium chloride (NaCl), ascorbic acid and sodium borohydride ($NaBH_4$) were purchased from Sinopharm Chemical Reagent Co., Ltd (Shanghai, China). Sodium dodecyl sulfate (SDS), was purchased from Alfa Aesar Co., Ltd (Tianjin, China).

All of the synthetic oligonucleotide sequences were purchased from Sangon Inc. (Shanghai, China), and their sequences are listed as follows:

Probe sequences: 5'-SH-$(CH_2)_6$-AAT GTA TAA TTG CGG GAC TCT AAT C-3'

Complementary sequences: 5'-GAT TAG AGT CCC GCA ATT ATA CAT T-3'

Single-base mismatched sequences: 5'-GAT TAG AGT CNC GCA ATT ATA CAT T-3'

("N" stands for A, T or G)

Non-complementary sequences: 5'-AGC CCA CAC TGA TGG CGC CAC TGC A-3'

All oligonucleotide stock solutions were prepared with 0.01 M phosphate buffered saline (PBS, pH 7.4) and stored in refrigerator. The buffers employed in this study were as follows: hybridization buffer solution (0.01 M PBS + 0.1 M NaCl, pH 7.4) and electrochemical test solution (0.1 M PBS, pH 7.4). All chemicals were of analytical grade and used without further purification. All solutions were prepared with twice-quartz-distilled water.

Apparatus

The UV-vis-NIR absorption spectra was taken on a U-3010 UV-vis-NIR spectrometer (Hitachi, Japan). Transmission electron microscope (TEM) (Hitachi-800) was used to obtain the image of the Au NRs. Scanning electron microscopy (SEM) (Hitachi JEOLJSM-6700 F, Japan) was used to obtain the morphologies of different materials.

Electrochemical measurements were performed using a CHI660A electrochemical workstation (Shanghai Chenhua Instruments Co., China). The three-electrode system consisted of a glassy carbon electrode (GCE) or the modified electrode as working electrode, a platinum wire as auxiliary electrode, and a saturated calomel electrode (SCE) as reference electrode.

Differential pulse voltammetry (DPV) was performed in a 10.0 mL electrochemical cell with 2.0 mL buffer solution, which were deoxygenated with nitrogen bubbling for at least 10 min and a nitrogen atmosphere was kept over the solution in electrochemical measurements. The experiment parameters were as follows: initial potential, 0.1 V; final potential, −0.65 V; pulse amplitudes, 0.05 V; pulse width, 0.05 s; sample width, 0.0167 s.

Preparation of Au NRs and Au NRs-GO nanocomposite

Au NRs were synthesized in aqueous solution according to the seed-mediated protocol [22]. Firstly, seed solution was prepared by reducing $HAuCl_4$ (2.5×10^{-4} M) with freshly prepared ice-cold $NaBH_4$ (5.0×10^{-3} M) in the presence of CTAB (0.10 M). After 2 h, the obtained solution was stored as the seed solution for the synthesis of Au NRs. Secondly, CTAB (5.0 mL, 0.20 M) was mixed with $AgNO_3$ solution (0.20 mL, 4.0×10^{-3} M) and $HAuCl_4$ (5.0 mL, 1.0×10^{-3} M) in

one flask at room temperature. Then 0.07 mL ascorbic acid (7.88×10^{-2} M) was added in the mixture solution with gentle stirring. After that, 12 μL of the seed solution was added to the growth solution to initiate the growth of Au NRs for 12 h (the solution temperature was kept at 30). Finally, excess CTAB was removed from the solution by centrifuging for 10 min at a rate of 8000 rpm, and the Au NRs were re-dispersed in distilled water. The Au NRs obtained were stored in refrigerator for further used.

Subsequently, 25 mg GO was dispersed in 10.0 mL water to obtain 2.5 mg mL^{-1} solution with the aid of ultrasonic agitation. Next, 50 μL GO was added to 1.0 mL Au NRs dispersion (GO:Au NRs = 1:20, v/v) and ultrasonic agitation for 10 min at room temperature. Thus, the Au NRs-GO nanocomposite was obtained.

Preparation of the DNA biosensor

Prior to modification, the bare glassy carbon electrode (GCE) was polished to a mirror-like surface with 1.0, 0.3 and 0.05 μm alumina powder, respectively. After that, the electrode was sequentially cleaned ultrasonically in 95% ethanol and twice-quartz-distilled water for 3 min. The electrode was dried in the nitrogen atmosphere.

5.0 μL of Au NRs-GO solution was dropped onto the surface of the pretreated GCE and dried naturally to form Au NRs-GO thin film at room temperature. The obtained electrode was denoted as Au NRs-GO/GCE.

4.0 μL of probe DNA (1.0×10^{-5} M) was dropped on the surface of Au NRs-GO/GCE and kept it in a refrigerator for 2 h. After that, the modified electrode was immersed in a 0.1% SDS for 5 min to remove the unbound probe DNA. Thus, the biosensor was obtained and denoted as ssDNA/Au NRs-GO/GCE.

Electrochemical detection of DNA hybridization

The ssDNA/Au NRs-GO/GCE was immersed into 0.01 M PBS containing complementary DNA for 40 min at 37 . It was then washed with 0.1% SDS and twice-quartz-distilled water three times to remove the unhybridized complementary DNA. Subsequently, it was incubated in

2.0×10^{-5} M MB solution for 20 min, followed by being washed with 0.1% SDS and distilled water. Then it was placed in electrolytic cell for electrochemical detection. Differential pulse voltammetry (DPV) was utilized to monitor the DNA hybridization event using MB as an electrochemical indicator. In this study, the peak current of MB ($\Delta I = I_{ds\text{-}DNA} - I_{ss\text{-}DNA}$) was used to quantify the concentration of complementary DNA. Here, $I_{ss\text{-}DNA}$ and $I_{ds\text{-}DNA}$ denote the reduction peak current of MB in absence and presence of the complementary DNA, respectively.

Results and discussion

Characteristics of Au NRs, Au NRs-GO nanocomposite and modified electrodes

The morphologies of different nanomaterials were obtained by SEM and TEM. As shown in Fig. 1A, the TEM image showed that the prepared-Au NRs present uniform shapes and sizes with an average diameter of 16 nm and an average length of 39 nm. Fig. 1B showed the UV-vis-NIR absorption spectra of Au NRs. It could be observed that Au NRs exhibit two distinct absorption bands at 510 and 746 nm, which were ascribed to transverse and longitudinal plasmon resonance absorption, respectively.

SEM images of the GO and Au NRs-GO nanomaterials were obtained and shown in Fig. 1C and 1D. It was obviously observed that the GO showed the typical crumpled and flake structure. With the addition of Au NRs, the dispersed Au NRs could self-assembly onto the surface of GO via electrostatic interaction.

Cyclic voltammetry was used to characterize the assembled process of the biosensor in 1.0 mM $[Fe(CN)_6]^{3-/4-}$ and the results shown in Fig. 1E. It was obviously observed that the peak current was largely decreased when GO was assembled on the surface of GCE (curve b) in contrast to the bare GCE (curve a); When Au NRs-GO nanocomposite was assembled on the surface of GCE, the peak current increased obviously (curve c), which indicates that Au NRs-GO is a kind of ideal electrical conducting material and accelerated the electron transfer of $[Fe(CN)_6]^{3-/4}$. When the probe DNA was assembled on the surface of the Au NRs-GO, the peak current decrease (curve d) and after the probe DNA hybridized with the target DNA, the peak current was continuously decrease (curve e). It was reasonable that probe DNA could block the electron transfer of

$[Fe(CN)_6]^{3-/4-}$ because they have negatively charged and appear the strong electrostatic repulsion interaction.

Fig. 1

Optimization of experimental conditions

We investigated the influence of incubation and hybridization time towards the performance of the biosensor. Fig. 2A showed the peak current of MB changed with the incubation time. It could be observed that the peak current of MB increased significantly with increasing incubation time from 5 min up to 20 min, and reached a platform after 20 min, suggesting most MB molecules have intercalated in dsDNA molecules after 20 min. Then the effect of DNA hybridization time on the peak current of MB was investigated. As shown in Fig. 2B, the peak current of MB obviously increased with increasing the hybridization time from 10 to 40 min, and remained stable after 40 min, indicating that the hybridization reaction was completed during 40 min. Thus, we chose the incubation time is 20 min and hybridization time is 40 min in subsequent experiments.

Fig. 2

Analytical performance of the biosensor

Under the optimal conditions, the analytical performance of the DNA biosensor was investigated. Fig. 3A showed that the reduction peak current of MB increased gradually with the increase of the concentration of complementary DNA. The peak currents of MB were linear with the logarithm of complementary DNA concentrations from 1.0×10^{-14} to 1.0×10^{-9} M with a detection limit of 3.5×10^{-15} M (S/N=3), as shown in Fig. 3B. The linear regression equation was $\Delta I = 35.974 + 2.496 \log c$, with a correlation coefficient of 0.995. Compared with the previously

similar works (seen in Table 1), the proposed biosensor showed lower detection limit and wider detection range for the complementary DNA detection than that of reported.

Fig. 3

Table 1

Selectivity of the biosensor

In addition of high sensitivity, the proposed biosensor possesses high specificity, enabling unambiguous discrimination of non-complementary, single-based mismatched (T, A and G) and complementary DNA sequence. As shown in Fig. 4A, the peak current of complementary DNA was larger (8.978×10^{-6} A) than non-complementary and single-based mismatched (T, A and G) DNA. The peak current of non-complementary and single-based mismatched (T, A and G) DNA is only were 11% , 33%, 37 %, and 35% of that produced by the complete complementary DNA at the same concentration, respectively (Fig. 4B), indicating that this biosensor has good selectivity.

To further assess the selectivity of this biosensor, we have design another approach to investigating the selectivity of the biosensor. This biosensor was employed to detect a series of solution containing various ratios of single-based mismatched (A) with complementary sequences (0:1, 1:1, 10:1, 100:1, 1000:1 and 1:0) and kept the total DNA concentration unchanged (1.0×10^{-9} M). As shown in Fig. 4C, it is obviously discriminated only complementary DNA (curve a) with only single-based mismatched DNA (curve f). Moreover, the peak current of MB decreased sharply with the ratio of two different DNA sequences from 1:1 to 10:1 and decreased slowly from 100:1 to 1000:1. More importantly, the complementary DNA can also be detected in the presence of a 1000-fold single-based mismatched DNA. All results showed that the biosensor can effectively discriminate the complementary DNA in presence of a large excess of the single-based mismatched DNA, suggesting this biosensor possesses excellent selectivity.

Fig. 4

Reproducibility and stability of DNA biosensor

The reproducibility of the DNA sensor was investigated. Five different biosensors were fabricated independently under the same conditions, and it was employed to detect 1.0×10^{-11} M complementary DNA. The current values obtained were 1.613×10^{-5}, 1.627×10^{-5}, 1.601×10^{-5}, 1.635×10^{-5}, 1.619×10^{-5} A, respectively. The relative standard deviation (R.S.D.) was 0.8 %, indicting that the biosensor has excellent reproducibility.

The stability of the biosensor was also investigated by detecting 1.0×10^{-11} M complementary DNA (measured everyday). As shown in Fig.5, it was observed no obviously changes (a ~ e) within one week. The relative standard deviation (R.S.D.) was 0.39 % ~ 0.73 %, shows indicating that the DNA biosensor possesses good stability.

Fig. 5

Conclusions

In this work, we reported a sensitive electrochemical biosensor for the detection of specific sequences DNA. This biosensor showed many advantages including simplicity, high sensitivity, excellent selectivity and good stability. It should be point out that the biosensor can effectively recognize the complementary DNA in a 1000-fold excess single-based mismatched DNA.

Acknowledgement

This work was financially supported by the National Natural Science Foundation of China (No. 20675002).

References

[1] J. Wang, Electrochemical biosensors: towards point-of-care cancer diagnostics, Biosens. Bioelectron. 21 (2006) 1887-1892.

[2]G.Chiti, G.Marrazza, M. Mascini, Electrochemical DNA biosensor for environmental monitoring, Anal. Chim. Acta 427 (2001) 155-164.

[3] H.Y. Liu, S.M. Xu, Z.M. He, A.P. Deng, J.J. Zhu, Supersandwich Cytosensor for Selective and Ultrasensitive Detection of Cancer Cells Using Aptamer-DNA Concatamer-Quantum Dots Probes, Anal. Chem. 85 (2013) 3385 3392.

[4] P. Liu, X.J. Li, S.A. Greenspoon, J.R. Scherer, R.A. Mathies, Integrated DNA purification, PCR, sample cleanup, and capillary electrophoresis microchip for forensic human identification, Lab Chip 11 (2011) 1041-1048.

[5] S.J. He, K.K. Liu, S. Su, J. Yan, X.H. Mao, D.F. Wang, Y. He, L.J. Li, S.P. Song, C.H. Fan, Graphene-based high-efficiency surface-enhanced Raman scattering-active platform for sensitive and multiplex DNA detection, Anal. Chem. 84 (2012) 4622-4627.

[6] Z.F. Ma, L. Tiana, T.T. Wang, C.G. Wang, Optical DNA detection based on gold nanorods aggregation, Anal. Chim. Acta 673 (2010) 179-184.

[7] X.Y. Dong, X.N. Mi, L. Zhang, T.M. Liang, J.J. Xu, H.Y. Chen, DNAzyme-functionalized Pt nanoparticles/carbon nanotubes for amplified sandwich electrochemical DNA analysis, Biosens. Bioelectron. 38 (2012) 337-341.

[8] D.C. Wang, L.H. Hu, H.M. Zhou, E.S. Abdel-Halim, J.J. Zhu, Molecular beacon structure mediated rolling circle amplification for ultrasensitive electrochemical detection of microRNA based on quantum dots tagging, Electrochem. Commun. 33 (2013) 80 – 83.

[9] F. Li, Y. Huang, Q. Yang, Z.T. Zhong, D. Li, L.H. Wang, S.P. Song, C.H. Fan, A graphene - enhanced molecular beacon for homogeneous DNA detection, Nanoscale 2 (2010) 1021-1026.

[10]J. Zhang, S.P. Song, L.H. Wang, D. Pan, C.H. Fan, A gold nanoparticle-based chronocoulometric DNA sensor for amplified detection of DNA, Nature 2 (2007) 2888-2895.

[11] J. Wang, A.N. Kawde, M. Musameh, Carbon-nanotube-modified glassy carbon electrodes for amplified label-free electrochemical detection of DNA hybridization, Analyst 128 (2003) 912-916.

[12] J.Wang, A.N. Kawde, A. Erdem, M. Salazar, Magnetic bead-based label-free electrochemical detection of DNA hybridization, Analyst 126 (2001) 2020-2024.

[13] J. Wang, S.J. Zhang, Y.Z. Zhang, Fabrication of chronocoulometric DNA sensor based on gold nanoparticles/poly(L-lysine) modified glassy carbon electrode, Anal. Biochem. 396 (2010) 304-309.

[14] J.J. Storhoff, R. Elghanian, R.C. Mucic, C.A. Mirkin, R. L. Letsinger, One-pot colorimetric differentiation of polynucleotides with single base imperfections using gold nanoparticle probes, J. Am. Chem. Soc. 120 (1998) 1959-1964.

[15] R. Elghanian, J.J. Storhoff, R.C. Mucic, R.L. Letsinger, C.A. Mirkin, Selective colorimetric detection of polynucleotides based on the distance-dependent optical properties of gold nanoparticles, Science 277 (1997) 1078-1081.

[16] C. Thiruppathiraja, S. Kamatchiammal, P. Adaikkappan, D. Jayakar Santhosh, M. Alagar, Specific detection of Mycobacterium sp. genomic DNA using dual labeled gold nanoparticle based electrochemical biosensor, Anal. Biochem. 417 (2011) 73-79.

[17] H.J. Paraba, C.Junga, J.H. Leeb, H.G. Park, A gold nanorods-based optical DNA biosensor for the diagnosis of pathogens, Biosens. Bioelectron. 26 (2010) 667-673.

[18] Z. Jia, J. Liu, Y.B. Shen, Fabrication of a template-synthesized gold nanorod-modified electrode for the detection of dopamine in the presence of ascorbic acid, Electrochem. Commun. 9 (2007) 2739-2743.

[19] Y.Y. Zhua, C.L. Qu, H. Kuang, L.G. Xu, L.Q. Liu, Y.F. Hua, L.B. Wang, C.L. Xu, Simple, rapid and sensitive detection of antibiotics based on the side-by-side assembly of gold nanorod probes, Biosens. Bioelectron. 26 (2011) 4387- 4392.

[20] C.Y. Denga, J.Z. Chen, M.H. Yang, Z. Nie, S.H. Si, Electrochemical determination of dopamine in the presence of ascorbic acid based on the gold nanorods/carbon nanotubes composite film, Electrochim. Acta 56 (2011) 8851- 8856.

[21] W. He, C.Z. Huang, Y.F. Li, J.P. Xie, R.G. Yang, P.F. Zhou, J. Wang, One-step label-free optical genosensing system for sequence-specific DNA related to the human immunodeficiency Virus based on the measurements of light scattering signals of gold nanorods, Anal. Chem. 80 (2008) 8424-8430.

[22] X..C. Lu, X. Dong, K.Y. Zhang, X.W. Han, X. Fang, Y. Z. Zhang, A gold nanorods-based

fluorescent biosensor for the detection of hepatitis B virus DNA based on fluorescence resonance energy transfer, Analyst 138 (2013) 642-650.

[23] H.F. Dong, W.C. Gao, F. Yan, H.X. Ji, H.X. Ju, Fluorescence resonance energy transfer between quantum dots and graphene oxide for sensing biomolecules, Anal. Chem. 82 (2010) 5511-5517.

[24] J. Zhang, Y. Sun, B. Xu, H.Zhang, Y. Gao, H.Q. Zhang, D.Q. Song, A novel surface plasmon resonance biosensor based on graphene oxide decorated with gold nanorod-antibody conjugates for determination of transferrin, Biosens. Bioelectron. 45 (2013) 230-236.

[25] X.L. Fua, L.X. Chen, J.H. Li, M. Lin, H.Y. You, W.H. Wang, Label-free colorimetric sensor for ultrasensitive detection of heparin based on color quenching of gold nanorods by graphene oxide, Biosens. Bioelectron. 34 (2012) 227-231.

[26] Y.Z. Zhang, W. Jiang, Decorating graphene sheets with gold nanoparticles for the detection of sequence-specific DNA, Electrochim. Acta. 71 (2012) 239 - 245.

[27] S. Radhakrishnan, C. Sumathi, V. Dharuman, J. Wilson, Polypyrrole nanotubes–polyaniline composite for DNA detection using methylene blue as intercalator, Anal. Methods 5 (2013) 1010-1015.

[28] X.W. Qi, H.W. Gao, Y.Y. Zhang, X.Z. Wang, Y. Chen, W. Sun, Electrochemical DNA biosensor with chitosan-Co_3O_4 nanorod-graphene composite for the sensitive detection of staphylococcus aureus nuc gene sequence, Bioelectrochemistry. 88 (2012) 42-47.

[29] L. Wang, L.Q. Lin, X.W. Xu, S.H. Weng, Y. Lei, A.L. Liu, Y.Z. Chen, X.H. Lin, Electrochemical biosensor for detection of PML/RAR fusion gene based on eriochrome cyanine R film modified glassy carbon electrode, Electrochim. Acta 69 (2012) 56-59.

[30] W. Sun, X.W. Qi, Y.Y. Zhang, H.R. Yang, H.W. Gao, Y. Chen, Z.F. Sun, Electrochemical DNA biosensor for the detection of Listeria monocytogenes with dendritic nanogold and electrochemical reduced graphene modified carbon ionic liquid electrode, Electrochim. Acta. 85 (2012) 145-151.

[31] S. Radhakrishnan, C.Sumathi, A. Umar, S.J. Kim, J.Wilson, V. Dharuman, Polypyrrole-poly (3,4-ethylenedioxythiophene)-Ag (PPy-PEDOT-Ag) nanocomposite films for label-free electrochemical DNA sensing, Biosens. Bioelectron. 47 (2013) 133-140.

[32] Y.W. Hu, S.C. Hua, F.H. Li, Y.Y. Jiang, X.X. Bai, D. Li, L. Niu, Green-synthesized gold nanoparticles decorated graphene sheets for label-free electrochemical impedance DNA hybridization biosensing, Biosens. Bioelectron. 26 (2011) 4355-4361.

Figure legends

Scheme. 1. Schematic representation of the DNA biosensor fabrication procedure.

Fig. 1. (A) TEM image of Au NRs; (B) UV–vis absorption spectrum of Au NRs; SEM images of (C) GO and (D) Au NRs-GO; (E) Cyclic voltammograms of 1.0 mM K3[Fe(CN)6] and 0.1 M KCl solution at different modified electrodes. From a to e were bare GCE, GO/GCE, Au NRs-GO/GCE, ssDNA/Au NRs-GO/GCE and dsDNA/Au NRs-GO/GCE, respectively.

Fig. 2. Optimization of the experimental conditions: (A) effect of DNA incubation time on DPV signals of the peak current of MB; (B) effect of DNA hybridization time on DPV signals of the peak current of MB ($C_{complementary\ DNA} = 1.0 \times 10^{-11}$ M, hybridization temperature: 37 , $C_{MB} = 2.0 \times 10^{-5}$ M).

Fig. 3. (A) DPV curves of the biosensor hybridized with increasing concentrations of complementary DNA:(a) 0 M; (b) 1.0×10^{-14} M; (c) 5.0×10^{-14} M; (d) 1.0×10^{-13} M; (e) 5.0×10^{-13} M; (f) 1.0×10^{-12} M; (g)1.0×10^{-11} M; (h) 1.0×10^{-10} M; (i) 1.0×10^{-9} M.

(B) Logarithmic plot of peak current of MB (Δ I) vs. the concentration of complementary DNA.

Fig. 4. (A) DPV responses of MB recorded after the biosensor (curve a) recognizing the various DNA sequences. Non-complementary DNA (curve b), single-base mismatched DNA (curve c, d, e) and complementary DNA (curve f). The concentration of different DNA sequences is 1.0×10^{-11} M.

(B) Histograms of the DPV signals of the biosensor recognized different DNA sequences.

(C) The histograms of the peak current response of the biosensor recognized different ratios of single-mismatched DNA with complementary DNA: (a) 0:1, (b) 1:1, (c) 10:1, (d) 100:1, (e) 1000:1 and (f) 1:0.

Fig. 5. The signal intensity obtained of five biosensors (a-e) within a week.

Table caption：

Table 1 Comparison of the performance of the different electrochemical DNA biosensors.

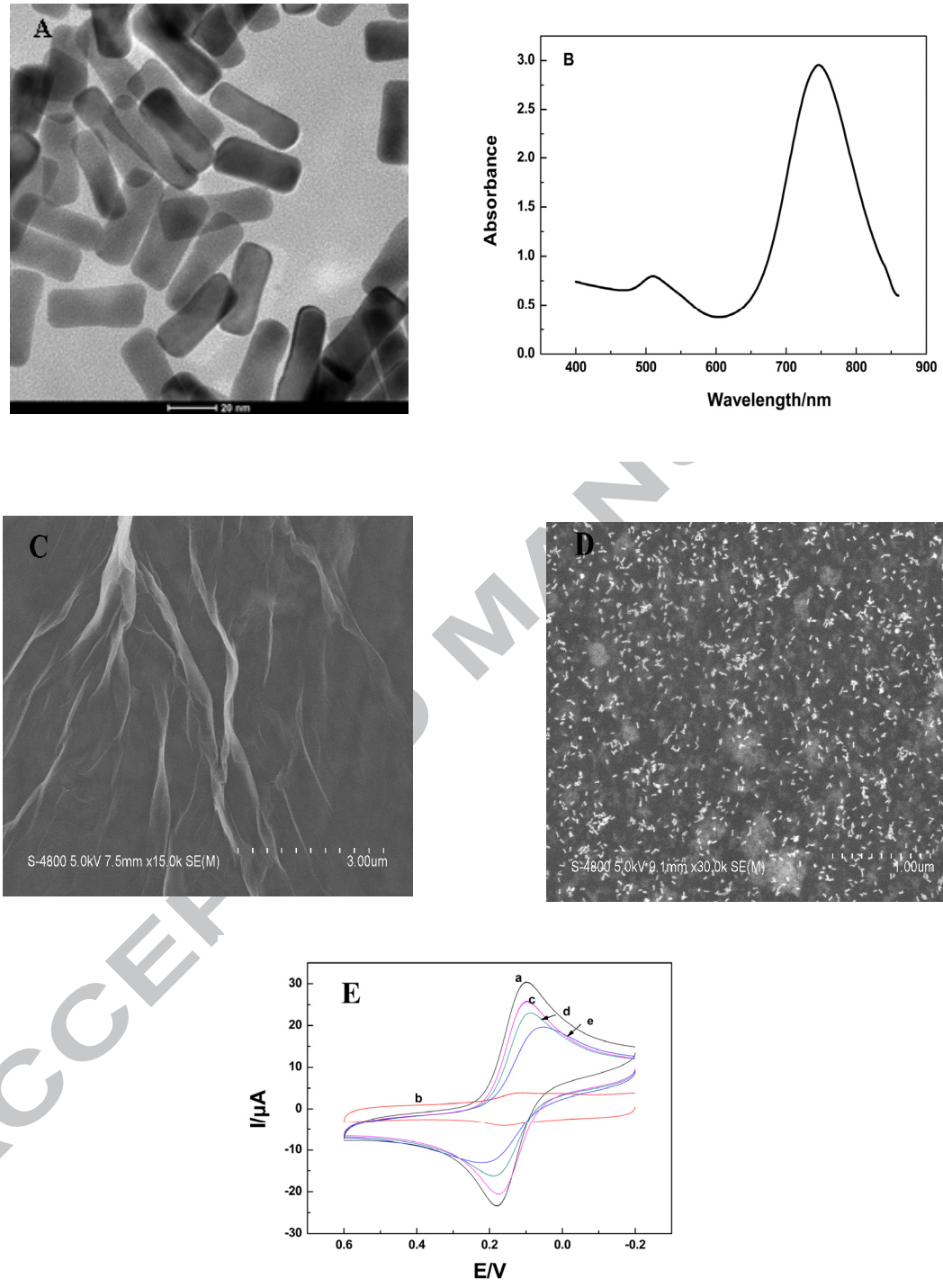
A
20 nm
B
Absorbance
Wavelength/nm
C
S-4800 5.0kV 7.5mm x15.0k SE(M)
3.00um
D
S-4800 5.0kV 9.1mm x30.0k SE(M)
1.00um
E
I/μA
E/V
a
b
c
d
e

Fig. 1

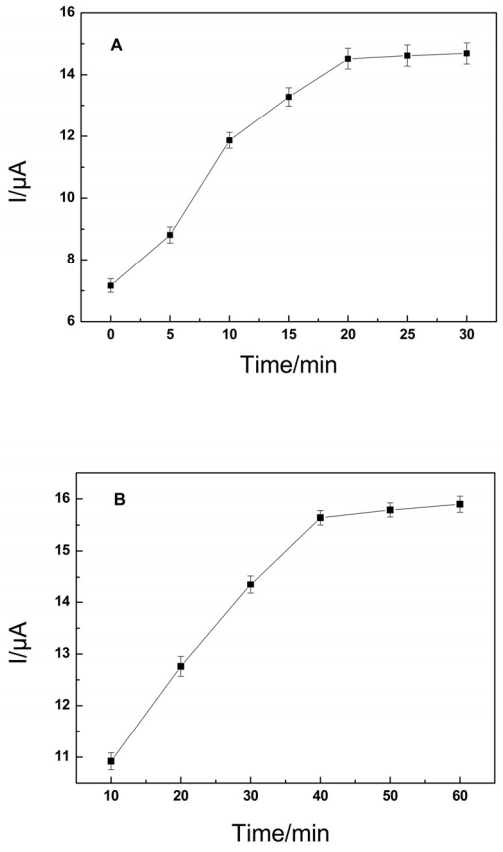

Fig. 2

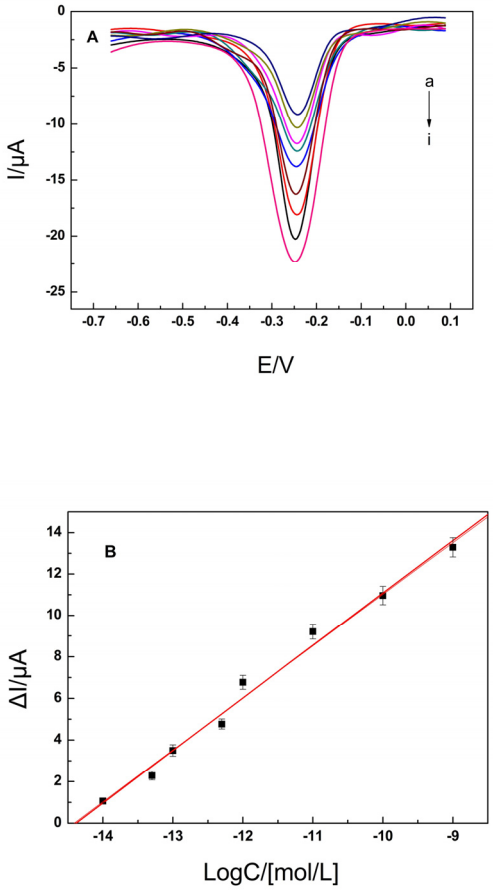

Fig. 3

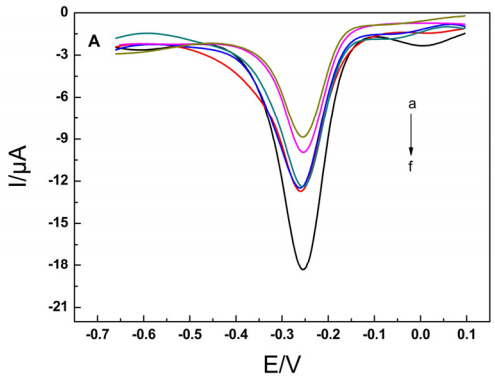

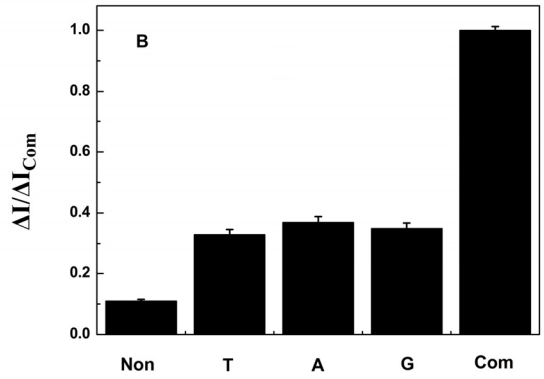

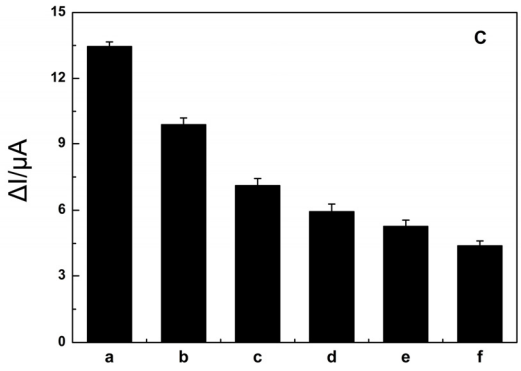

Fig. 4

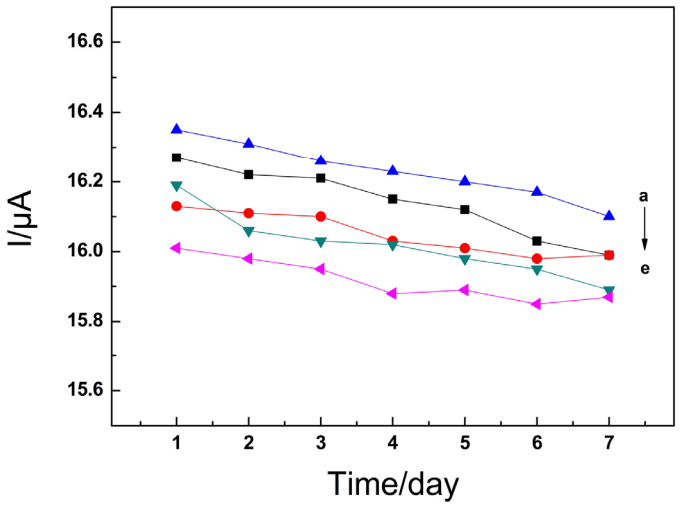

Fig. 5

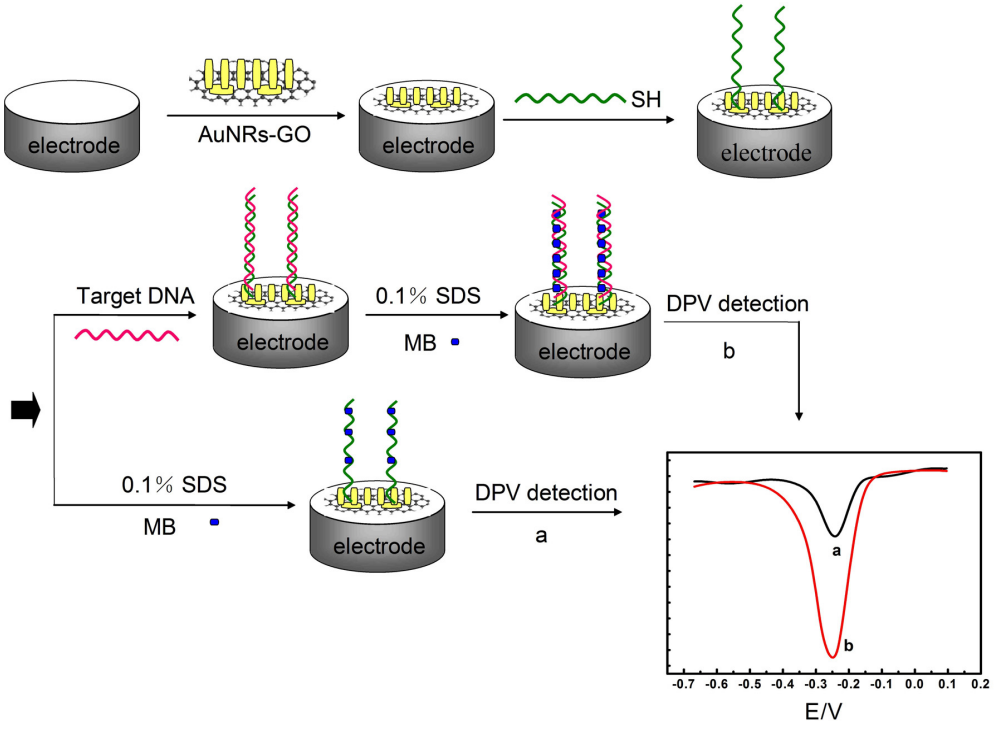

Scheme 1.

Table 1

Electrodes	Indicators	Methods	Linear range (M)	Detection limit (M)	References
AuNPs/rGO/GCE	Adriamycin	DPV	1.0×10^{-13}—1.0×10^{-8}	3.5×10^{-14}	[26]
PPy–PANi–GA/GE	MB	DPV	1.0×10^{-13}—1.0×10^{-9}	5.0×10^{-14}	[27]
CTS–Co_3O_4–GR/CILE	MB	DPV	1.0×10^{-12}—1.0×10^{-6}	4.3×10^{-13}	[28]
ECR /GCE	MB	DPV	5.0×10^{-12}—2.0×10^{-10}	9.8×10^{-11}	[29]
MAA/Au/GR/CILE	MB	DPV	1.0×10^{-12}—1.0×10^{-6}	2.9×10^{-13}	[30]
PPy–PEDOT–Ag /GCE	—	EIS	1.0×10^{-14}—1.0×10^{-11}	5.4×10^{-15}	[31]
Au-IL/PTCA/graphene /GCE	—	EIS	1.0×10^{-13}—1.0×10^{-6}	3.4×10^{-14}	[32]
AuNRs-GO/GCE	MB	DPV	1.0×10^{-14}—1.0×10^{-9}	3.5×10^{-15}	This work

Note. rGO, reduced graphene oxide; PPy, polypyrrole; PANi, polyaniline; GA, gluteraldehyde; GE, gold electrode; CTS, chitosan; GR, graphene; CILE, carbon ionic liquid electrode; ECR, eriochrome cyanine R; MAA, Mercaptoacetic acid; PPy-PEDOT, polypyrrole and poly(3,4-ethylenediox-ythiophene); Au-IL, NH2-IL stabilized gold nanoparticles; PTCA, 3,4,9,10-perylene tetracarboxylic acid.